

THE GAMMA RAY BURST LUMINOSITY FUNCTION IN THE LIGHT OF THE *SWIFT* 2-YEAR DATAR. SALVATERRA,<sup>1</sup> G. CHINCARINI,<sup>1,2</sup>*Draft version September 23, 2018*

## ABSTRACT

We compute the luminosity function (LF) and the formation rate of long gamma ray bursts (GRBs) by fitting the observed differential peak flux distribution obtained by the *BATSE* satellite in three different scenarios: i) GRBs follow the cosmic star formation and their LF is constant in time; ii) GRBs follow the cosmic star formation but the LF varies with redshift; iii) GRBs form preferentially in low-metallicity environments. We find that the differential peak flux number counts obtained by *BATSE* and by *Swift* can be reproduced using the same LF and GRB formation rate, indicating that the two satellites are observing the same GRB population. We then check the resulting redshift distributions in the light of *Swift* 2-year data, focusing in particular on the relatively large sample of GRBs detected at  $z > 2.5$ . We show that models in which GRBs trace the cosmic star formation and are described by a constant LF are ruled out by the number of high- $z$  *Swift* detections. This conclusion does not depend on the redshift distribution of bursts that lack of optical identification, nor on the existence of a decline in star formation rate at  $z > 2$ , nor on the adopted faint-end of the GRB LF. *Swift* observations can be explained by assuming that the LF varies with redshift and/or that GRB formation is limited to low-metallicity environments.

*Subject headings:* gamma-ray: burst – stars: formation – cosmology: observations.

## 1. INTRODUCTION

Gamma Ray Bursts (GRBs) are powerful flashes of high-energy photons occurring at an average rate of a few per day throughout the universe. Even though they are highly transient events very hard to localize, they are so bright that they can be detected up to very high redshift (the current record is  $z = 6.29$ ). The energy source of a GRB is believed to be associated to the collapse of the core of a massive star in the case of long-duration GRBs, and due to merger- or accretion-induced collapse for the short-hard class of GRBs (see Mészáros 2006 for a recent review). In this paper, we limit our analysis to the class of long-duration GRBs.

One of the main goals of the *Swift* satellite (Gehrels et al. 2004) is to tackle the key issue of the GRB luminosity function (LF). Unfortunately, although the number of GRBs with good redshift determination has been largely increased by *Swift*, the sample is still too poor (and bias dominated) to allow a direct measurement of the LF. Many studies (e.g. Lamb & Reichart 2000; Porciani & Madau 2001 (PM01); Schmidt 2001; Choudhury & Srianand 2002; Firmani et al. 2004; Guetta, Piran & Waxman 2005; Natarajan et al. 2005; Daigne, Rossi & Mochkovitch 2006) tried to constrain the GRB LF under the assumption that GRBs trace the observed star formation rate, as suggested by the association of long GRBs to the death of massive stars. Following these works and assuming the most recent star formation rate determination, we derive the LF and formation rate of GRBs by fitting the observed *BATSE* differential peak flux distribution in three different scenarios: i) GRBs follow the cosmic star formation and have a constant LF; ii) the

GRB LF varies with redshift; iii) GRBs form in low-metallicity environments. We check the results against the 2-year *Swift* data, focusing in particular on the large sample of high redshift ( $z > 2.5$ ) GRBs detected by this instrument.

## 2. BASIC EQUATIONS

The observed photon flux,  $P$ , in the energy band  $E_{\min} < E < E_{\max}$ , emitted by an isotropically radiating source at redshift  $z$  is

$$P = \frac{(1+z) \int_{(1+z)E_{\min}}^{(1+z)E_{\max}} S(E) dE}{4\pi d_L^2(z)}, \quad (1)$$

where  $S(E)$  is the differential rest-frame photon luminosity of the source, and  $d_L(z)$  is the luminosity distance. To describe the typical burst spectrum we adopt the functional form proposed by Band et al. (1993), i.e. a broken power-law with a low-energy spectral index  $\alpha$ , a high-energy spectral index  $\beta$ , and a break energy  $E_b$ . In this work, we take  $\alpha = -1$  and  $\beta = -2.25$  (Preece et al. 2000), and  $E_b = 511$  keV (PM01). Moreover, it is customary to define an isotropic equivalent intrinsic burst luminosity in the energy band 30-2000 keV as  $L = \int_{30\text{keV}}^{2000\text{keV}} ES(E) dE$ . Given a normalized GRB LF,  $\phi(L)$ , and the detector efficiency,  $\epsilon(P)$ , the observed rate of bursts with peak flux between  $P_1$  and  $P_2$  is

$$\frac{dN}{dt}(P_1 < P < P_2) = \int_0^\infty dz \frac{dV(z)}{dz} \frac{\Delta\Omega_s}{4\pi} \frac{\Psi_{\text{GRB}}(z)}{1+z} \times \int_{L(P_1, z)}^{L(P_2, z)} dL' \phi(L') \epsilon(P), \quad (2)$$

where  $dV(z)/dz = 4\pi c d_L^2(z)/[H(z)(1+z)^2]$  is the comov-

<sup>1</sup> Dipartimento di Fisica G. Occhialini, Università degli Studi di Milano Bicocca, Piazza della Scienza 3, I-20126 Milano, Italy, salvaterra@mib.infn.it

<sup>2</sup> INAF, Osservatorio Astronomico di Brera, via E. Bianchi 46, I-23807 Merate (LC), Italy

ing volume element<sup>3</sup>, and  $H(z) = H_0[\Omega_M(1+z)^3 + \Omega_\Lambda + (1-\Omega_M-\Omega_\Lambda)(1+z)^2]^{1/2}$ .  $\Delta\Omega_s$  is the solid angle covered on the sky by the survey, and the factor  $(1+z)^{-1}$  accounts for cosmological time dilation. Finally,  $\Psi_{\text{GRB}}(z)$  is the comoving burst formation rate. In this work, we assume that the GRB LF is described by

$$\phi(L) \propto \left(\frac{L}{L_{\text{cut}}}\right)^{-\xi} \exp\left(-\frac{L_{\text{cut}}}{L}\right). \quad (3)$$

### 3. MODELS

We consider three different scenarios. In the first one, the GRB formation rate is proportional to the cosmic star formation rate (SFR),  $\Psi_\star(z)$ , i.e.  $\Psi_{\text{GRB}}(z) = k_{\text{GRB}}\Psi_\star(z)$ , and the LF does not evolve with redshift, i.e.  $L_{\text{cut}} = \text{const} = L_0$ . The factor  $k_{\text{GRB}}$  gives the number of GRBs formed per solar mass in stars and has units of  $\text{M}_\odot^{-1}$ .  $\Psi_\star(z)$  (in units of  $\text{M}_\odot \text{Mpc}^{-3} \text{yr}^{-1}$ ) is commonly parameterized with the form proposed by Cole et al. (2001) as

$$\Psi_\star(z) = \frac{(a_1 + a_2 z)h}{1 + (z/a_3)^{a_4}}. \quad (4)$$

Recently, Hopkins & Beacom (2006) have provided the values of the coefficients  $a$  by fitting the available UV and far-infrared measurements for  $z < 6$ , corrected for dust obscuration. In this paper, we adopt their best fit parameters:  $a_1 = 0.017$ ,  $a_2 = 0.13$ , and  $a_3 = 3.3$  (Hopkins & Beacom 2006). The value of  $a_4 = 4.3$  is taken to be slightly lower than the original one in order to match the decline of the SFR with  $(1+z)^{-3.3}$  at  $z \gtrsim 5$  suggested by recent deep-field data (see Stark et al. 2006 and references therein).

In the second scenario, while the GRB formation rate is still proportional to the observed SFR, the cut-off luminosity in the GRB LF increases with redshift as  $L_{\text{cut}} = L_0(1+z)^\delta$ . Lloyd-Ronning, Fryer & Ramirez-Ruiz (2002), using GRB redshifts and luminosities derived from the luminosity-variability relationship, found that the data imply  $\delta \simeq 1.4 \pm 0.5$ , and we adopt this as fiducial value.

Finally, we consider a case in which GRBs form only in environments with metallicity below a given threshold (no evolution in the LF is considered). In fact, some theoretical models (see Mészáros 2006 and reference therein) require that GRB progenitors should have metallicity  $\lesssim 0.1 Z_\odot$ . Observations of GRB host galaxies (see Savaglio 2006 and reference therein) seems in agreement with this prescription, showing that GRB preferentially originates in low-metallicity regions. Langer & Norman (2006) have quantified the amount of star formation at a given metallicity, using a recent determination of the stellar mass function (Panter et al. 2004) and the observed mass-metallicity correlation (Savaglio et al. 2005). Adopting the metallicity redshift evolution derived from emission line studies (Kewley & Kobulnicky 2005), the fractional mass density belonging to metallicity below a given threshold,  $Z_{th}$ , can be computed as

$$\Sigma(z) = \frac{\hat{\Gamma}(0.84, (Z_{th}/Z_\odot)^2 10^{0.3z})}{\Gamma(0.84)}, \quad (5)$$

where  $\hat{\Gamma}$  ( $\Gamma$ ) are the incomplete (complete) gamma function, and  $\Gamma(0.84) \simeq 1.122$ . The GRB formation rate is then given by  $\Psi_{\text{GRB}}(z) = k_{\text{GRB}}\Sigma(z)\Psi_\star(z)$ . The main effect of this convolution is that the GRB formation rate peaks at higher redshift with respect to the cosmic SFR. We adopt  $Z_{th} = 0.1 Z_\odot$  as fiducial value, and, in this case, the GRB formation peaks at  $z \sim 3.5$ .

### 4. GRB NUMBER COUNTS

The free parameters in our model are the GRB formation efficiency  $k_{\text{GRB}}$ , the cut-off luminosity at  $z = 0$ ,  $L_0$ , and the power index,  $\xi$ , of the GRB LF function. Following PM01, we optimized the value of these parameters by  $\chi^2$  minimization over the observed differential number counts in the 50–300 keV band of *BATSE*. We use the off-line *BATSE* sample of Kommers et al. (2000), which includes 1998 archival (“triggered” plus “non-triggered”) bursts, and for which the detector efficiency is well described by the function  $\epsilon(P) = 0.5[1 + \text{erf}(-4.801 + 29.868P)]$  (Kommers et al. 2000). We report the best-fit parameters for our fiducial models in Table 1. In the last column, we give the reduced  $\chi^2$  for the best-fitting model, showing that it is always possible to find a good agreement with the data<sup>4</sup>. Note that for the metallicity evolution scenario a higher GRB formation efficiency is required, since GRBs form only in a (small) fraction of star forming galaxies.

We can now use the best-fit parameters to compute the expected differential peak flux distribution of GRBs in the 15–150 keV band of the Burst Alert Telescope (BAT) instrument onboard of *Swift*. The results are plotted in Figure 1 and compared with the observed *Swift*/BAT data points. All models show a good agreement with the data without the need of any change of the GRB LF and formation efficiency, indicating that *BATSE* and *Swift* are observing essentially the same population of GRBs. This conclusion is rather insensitive to 20% variations of the adopted GRB spectrum parameters, i.e. for the large majority of burst spectra (Kaneko et al. 2006).

### 5. GRB REDSHIFT DISTRIBUTION

Our model allows us to compute the expected redshift distribution of GRBs detected by *Swift*. We decide to avoid the comparison between model results and the overall observed distribution of bursts with known redshift, since this procedure implicitly assumes that the observed sample of GRBs with redshift determination is representative of all detected sources. Moreover, important information are missed by this kind of analysis: for example, that many bright GRBs are identified at high redshift. So, we try to answer this simple question: *is the redshift distribution consistent with the number of Swift detections at  $z > 2.5$  and  $z > 3.5$ ?*

The cumulative number of GRBs, identified during the two years of the *Swift* mission at  $z > 2.5$  (left panel) and  $z > 3.5$  (right panel), is plotted in Figure 2 together with model predictions. Note that *Swift* detections are

<sup>3</sup> We adopted the ‘concordance’ model values for the cosmological parameters:  $h = 0.7$ ,  $\Omega_m = 0.3$ , and  $\Omega_\Lambda = 0.7$ .

<sup>4</sup> Note that strong covariance on  $L_0$  and  $\xi$  is observed in the parameter space surrounding the best-fit parameters (see also PM01)

to be considered as a strong lower limit, since many high- $z$  bursts can be missed by optical follow-up searches.

The model with no LF evolution clearly underestimates the number of high redshift GRB detections at any photon flux and no bright GRBs are predicted for  $z > 3.5$ . We checked that variations of the shape of the SFR do not affect this result: even assuming a constant SFR at  $z \gtrsim 2$ , the model predictions do not change significantly. In fact, for relatively bright GRBs, the rapid decline in the LF strongly hampers the detection of high redshift bursts. Furthermore, our analysis does not depend on the faint-end of the LF: increasing the population of faint GRBs would decrease the number of high- $z$  detections, strengthening our conclusion. So, models in which GRBs trace the cosmic SFR and are described by a constant LF, are ruled out by the large sample of high- $z$  *Swift* GRBs.

The number of high- $z$  *Swift* identifications can be justified assuming that the LF varies with redshift. In this case, high- $z$  GRBs are typically brighter than low- $z$  ones, so that are much easily detected. Assuming that the luminosity increases as  $(1+z)^{1.4}$ , we find many sources at  $z > 2.5$ , but the model is barely consistent with the number of bright GRBs at  $z > 3.5$ . Since some high- $z$  sources can be missed by optical follow-up searches, an even stronger evolution might be required to explain the data.

Finally, we consider the possibility that GRB formation is restricted to low-metallicity environments. In this case, the peak of the GRB formation is shifted towards higher redshift, so that the probability of high- $z$  detections increases. Assuming  $Z_{th} = 0.1 Z_{\odot}$ , *Swift* identification are exceeded both at  $z > 2.5$  and  $z > 3.5$  without requiring any evolution in the LF. Thus, the model is consistent with a fraction of high redshift bursts missed by optical follow-up searches. Increasing the threshold metallicity will decrease the number of sources at high- $z$ : for  $Z_{th} \sim 0.4 Z_{\odot}$  the model becomes inconsistent with the number of observed GRBs at  $z > 3.5$ . Higher threshold values would require evolution of the GRB luminosity and/or a more gentle decline of the SFR at high redshift.

In conclusion, the existence of a large sample of bursts at  $z > 2.5$  in the *Swift* 2-year data imply that GRBs have experienced some kind of evolution, being more luminous or more common in the past.

## 6. GRB RATE AT REDSHIFT LARGER THAN SIX

The discovery of GRB050904 at  $z = 6.29$  (Antonelli et al. 2005; Tagliaferri et al. 2005; Kawai et al. 2006) during the first year of the *Swift* mission has strengthened the idea that many GRBs should be observed out to very high redshift (e.g. Natarajan et al. 2005; Bromm & Loeb 2006; Daigne et al. 2006). Unfortunately, no other source at  $z \gtrsim 6$  has been detected in the second year of observations.

In Figure 3, we plot the *Swift* detection rate expected for the three scenarios here considered. Models without evolution predict almost no sources to be detected at very

high redshift. If luminosity evolution ( $\delta = 1.4$ ) is allowed,  $\sim 2$  bursts/yr should lie above  $z \sim 6$  for  $P > 0.2$  ph cm $^{-2}$  s $^{-1}$ , whereas, in the metallicity evolution scenario ( $Z_{th} = 0.1 Z_{\odot}$ ), we expect  $\sim 8$  GRBs/yr, one or two being at  $z \gtrsim 8$ .

The detection rate are found to decrease rapidly with increasing peak fluxes. Indeed, it is interesting to note that GRB050904 was relatively bright, being its observed photon flux  $P = 0.658$  ph cm $^{-2}$  s $^{-1}$ . At this limit, only  $\sim 1$  (2) bursts/yr would be at  $z \gtrsim 6$ , if luminosity (metallicity) evolution is assumed. Thus, the lack of very high redshift identification in the 2nd year of the *Swift* mission might be due to practical difficulties in the optical follow-up of faint GRBs. In fact, no GRB with observed photon fluxes below  $0.5$  ph cm $^{-2}$  s $^{-1}$  has UVOT detection and only in a couple of cases a reliable redshift determination was possible. So, the identification of just one burst at  $z \gtrsim 6$  in two years of *Swift* mission is not very surprising. On the contrary, the discovery of GRB050904 may suggest that the *Swift* follow-up procedure is working very well, at least for relatively bright bursts.

## 7. CONCLUSIONS

We have computed the luminosity function and the formation rate of long GRBs by fitting the *BATSE* differential peak flux number counts in three different scenarios: i) GRBs follow the cosmic star formation and have a redshift-independent LF; ii) the GRB LF varies with redshift; iii) GRBs are associated with star formation in low-metallicity environments. In all cases, it is possible to obtain a good fit to the data by adjusting the model free parameters. Moreover, using the same LF and formation rate, it is possible to reproduce both *BATSE* and *Swift* differential counts, showing that the two satellites are observing the same GRB population.

We have then computed the expected burst redshift distribution, testing the results against the number of high redshift GRBs, detected during the two years of the *Swift* mission. We find that models where GRBs trace the SFR and are described by a constant LF largely underestimate the number high- $z$  GRBs detected by *Swift*. This conclusion does not depend on the redshift distribution of burst lacking of optical identification, nor on the existence of a decline in the SFR at  $z > 2$ , nor on the adopted faint-end of the LF. Alternatively, we find that the observed number of high- $z$  detection can be justified by assuming that the GRB luminosity increases with redshift and/or that GRBs preferentially form in low-metallicity environments.

Finally, we have estimated the detection rate of bursts at very high redshift. We find that  $\sim 2$  (8) GRBs/yr should be observed at  $z \gtrsim 6$ , if luminosity (metallicity) evolution is assumed. The majority of these sources is faint and may be missed in optical follow-up searches, but  $\sim 1$  (3) GRB/yr should be relatively bright, with an observed photon flux in excess to  $0.5$  ph cm $^{-2}$  s $^{-1}$ .

## REFERENCES

- Antonelli, L. A., et al. 2005, GNC, 3924, 1
- Band, D., et al. 1993, ApJ, 413, 281
- Bromm, V., & Loeb, A. 2006, ApJ, 642, 382
- Choudhury, T. R., & Srianand, R. 2002, MNRAS, 336, 27
- Cole, S., et al. 2001, MNRAS, 326, 255
- Daigne, F., Rossi, E. M., & Mochkovitch, R. 2006, MNRAS, 372, 1034

- Firmani, C. Avila-Reese, V., Ghisellini, G., & Tutukov, A. V. 2004, *ApJ*, 611, 1033
- Gehrels, N., et al. 2004, *ApJ*, 611, 1005
- Guetta, D., Piran, T., & Waxman, E. 2005, *ApJ*, 619, 412
- Hopkins, A. M., & Beacom, J. F. 2006, *ApJ*, 651, 142
- Kaneko, Y., Preece, R. D., Briggs, M. S., Paciesas, W. S., Meegan, C. A., & Band, D. L., 2006, *ApJS*, 166, 298
- Kawai, N., et al. 2006, *Nature*, 440, 184
- Kewley, L., & Kobulnicky, H.A. 2005, in: *Starburst: From 30 Doradus to Lyman Break Galaxies*, R. de Grijs and R. M. Gonzalez Delgado, Astrophysics & Space Science Library, Vol. 329. Dordrecht: Springer, p. 307
- Kommers, J. M., Lewin, W. H. G., Kouveliotou, C., van Paradijs, J., Pendleton, G. N., Meegan, C. A., & Fishman, G. J. 2000, *ApJ*, 533, 696
- Lamb, D. Q., & Reichart, D. E. 2000, *ApJ*, 536, 1
- Langer, L., & Norman, C. A. 2006, *ApJ*, 638, L63
- Lloys-Ronning, N. M., Fryer, C. L., & Ramirez-Ruiz, E. 2002, *ApJ*, 574, 554
- Mészáros, P. 2006, *Reports of Progress in Physics*, 69, 2259
- Natarajan, P., Albanna, B., Hjorth, J., Ramirez-Ruiz, E., Tarvir, N., & Wijers, R. 2005, *MNRAS*, 364, L8
- Panther, B., Heavens, A. F., & Jimenez, R. 2004, *MNRAS*, 355, 764
- Porciani, C., & Madau, P. 2001, *ApJ*, 548, 522 (PM01)
- Preece, R. D., Briggs, M. S., Mallozzi, R. S., Pendleton, G. N., Paciesas, W. S., & Band, D. L. 2000, *ApJS*, 126, 19
- Savaglio, S., et al. 2005, *ApJ*, 635, 260
- Savaglio, S. 2006, *NJPh*, 8, 195
- Schmidt, M. 2001, *ApJ*, 552, 36
- Stark, D. P., Bunker, A. J., Ellis, R. S., Eyles, L. P., & Lacy, M. 2006, *ApJ* in press, astro-ph/0604250
- Tagliaferri, G., et al. 2005, *A&A*, 443, L1

TABLE 1  
BEST FIT PARAMETERS FOR DIFFERENT MODELS. ERRORS ARE AT  $1\sigma$  LEVEL.

Model	$k_{\text{GRB}}/(10^{-8}\text{M}_{\odot}^{-1})$	$L_0/(10^{51}\text{erg s}^{-1})$	$\xi$	$\chi_r^2$
no evolution	$1.14 \pm 0.07$	$9.54 \pm 4.55$	$3.54 \pm 0.78$	0.83
luminosity evolution ( $\delta = 1.4$ )	$1.05 \pm 0.05$	$0.77 \pm 0.13$	$2.19 \pm 0.95$	0.80
metallicity evolution ( $Z_{th} = 0.1 Z_{\odot}$ )	$10.0 \pm 0.5$	$16.7 \pm 5.7$	$2.94 \pm 0.34$	0.84

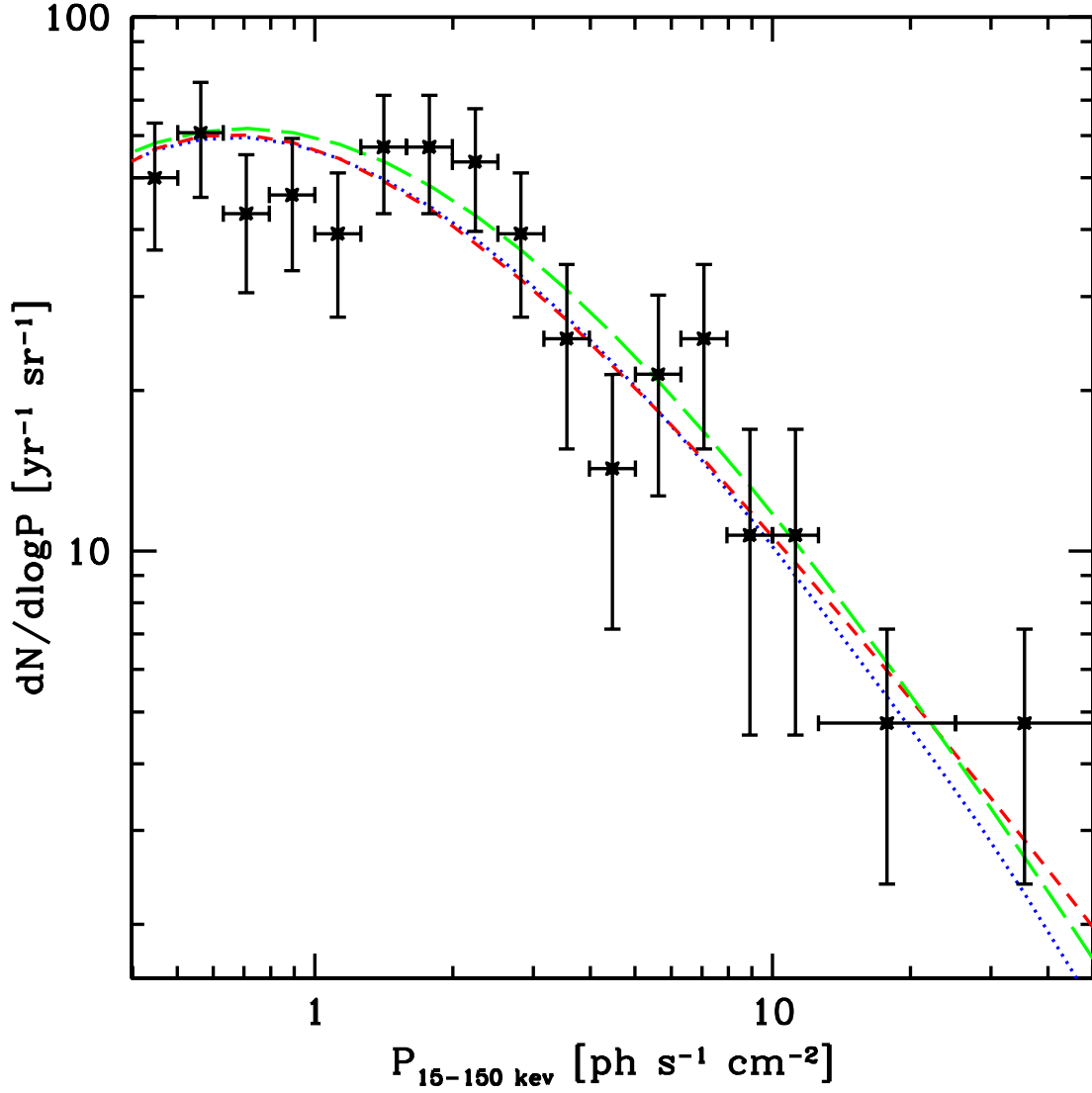


FIG. 1.— Differential number counts for *Swift* in the 15–150 keV band as a function of the observed photon flux  $P$ . The points show the observed counts and their Poisson uncertainties (horizontal error bars denote bin size). Dotted lines refers to the model without evolution, short-dashed line to the luminosity evolution model ( $\delta = 1.4$ ), and long-dashed line to the model with the metallicity threshold for GRB formation ( $Z_{th} = 0.1 Z_{\odot}$ ). A field of view of 1.4 sr for *Swift*/BAT is adopted.

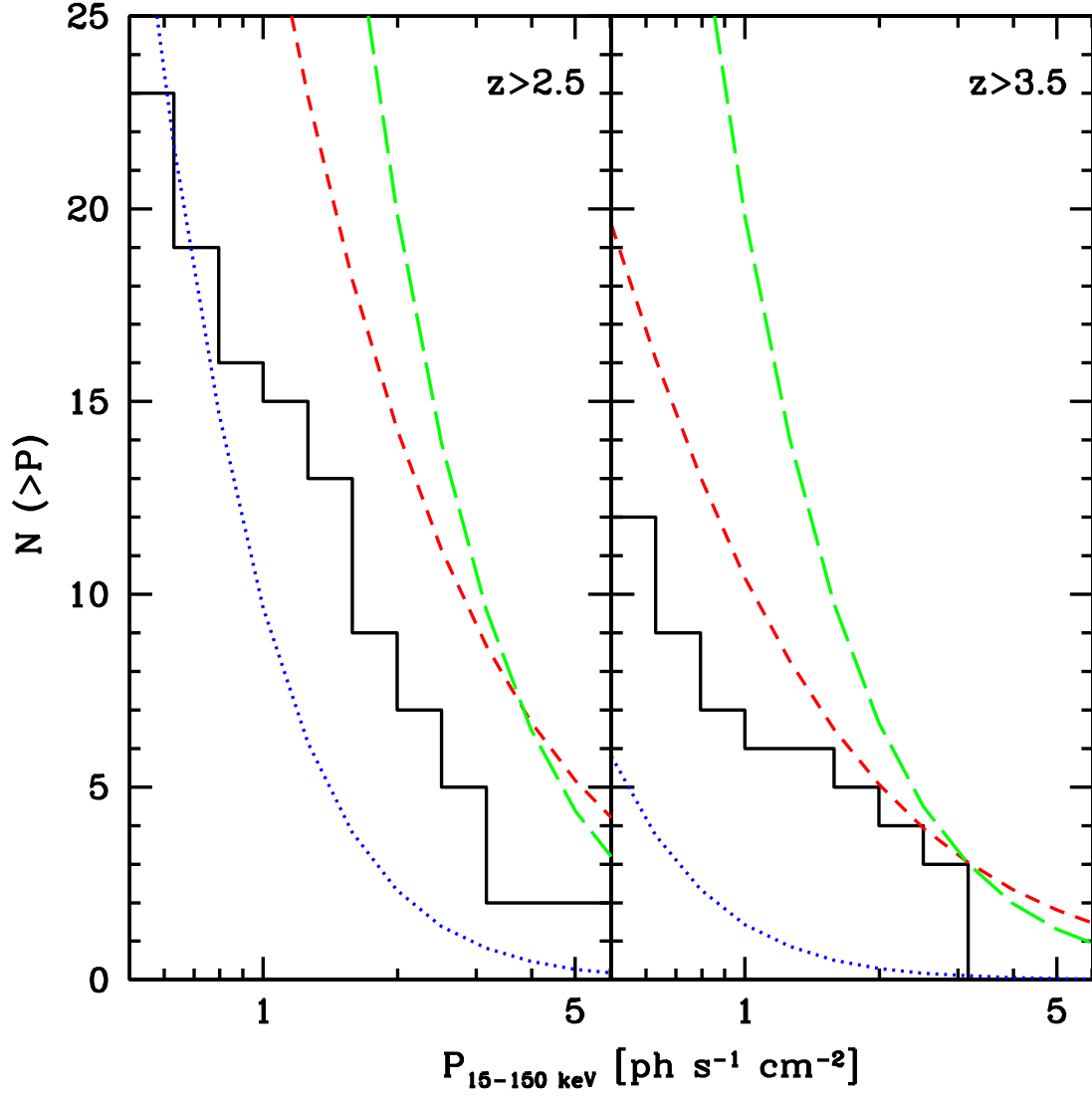


FIG. 2.— Cumulative number of high redshift GRBs at  $z > 2.5$  (right panel) and at  $z > 3.5$  (left panel) as a function of the observed photon flux  $P$  in the 15–150 keV band. The number of sources detected in the two years of *Swift* mission is shown as solid histogram, whereas model results are shown with lines as in the previous figure. Note that the observed detections are lower limits, since many high- $z$  GRBs can be missed by optical follow-up searches. A field of view of 1.4 sr for *Swift*/BAT is adopted.

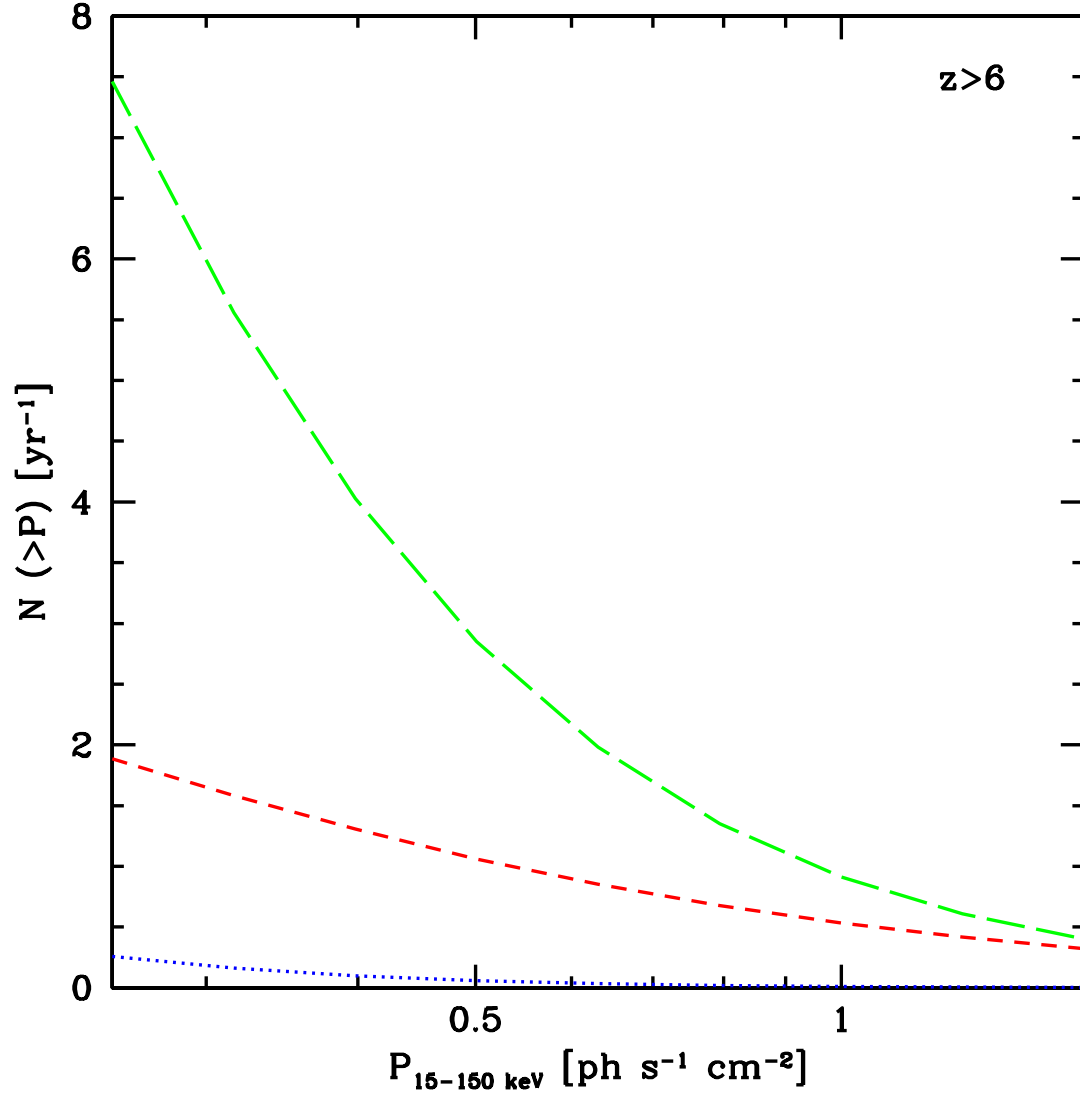


FIG. 3.— Cumulative rate of  $z \gtrsim 6$  GRBs detectable by *Swift* as a function of the photon flux  $P$ . A field of view of 1.4 sr for *Swift*/BAT is adopted. Lines as in Figure 1.